Aalto University

OPEN ACCESS

This is an electronic reprint of the original article.
This reprint may differ from the original in pagination and typographic detail.

Pälli, Samu Ville; Tamminen, Aleksi; Hiltunen, Paavo; Rexhepi, Sazan; Bonmann, Marlene; Bryllert, Tomas; Robertson, Duncan A.; Ala-Laurinaho, Juha; Stake, Jan; Taylor, Zachary

Imaging experiments with a 340-GHz FMCW radar and frequency-diverse holograms

Published in:
Radar Sensor Technology XXVII

DOI:
10.1117/12.2663757

Published: 01/01/2023

Document Version
Publisher's PDF, also known as Version of record

Please cite the original version:
Pälli, S. V., Tamminen, A., Hiltunen, P., Rexhepi, S., Bonmann, M., Bryllert, T., Robertson, D. A., Ala-Laurinaho, J., Stake, J., & Taylor, Z. (2023). Imaging experiments with a 340-GHz FMCW radar and frequency-diverse holograms. In A. S. Hedden, G. J. Mazzaro, & A. M. Raynal (Eds.), *Radar Sensor Technology XXVII* Article 125350M (Proceedings of SPIE - The International Society for Optical Engineering; Vol. 12535). SPIE. https://doi.org/10.1117/12.2663757

This material is protected by copyright and other intellectual property rights, and duplication or sale of all or part of any of the repository collections is not permitted, except that material may be duplicated by you for your research use or educational purposes in electronic or print form. You must obtain permission for any other use. Electronic or print copies may not be offered, whether for sale or otherwise to anyone who is not an authorised user.

PROCEEDINGS OF SPIE

SPIEDigitalLibrary.org/conference-proceedings-of-spie

Imaging experiments with a 340-GHz FMCW radar and frequency-diverse holograms

Samu-Ville Pälli, Aleksi Tamminen, Paavo Hiltunen, Sazan Rexhepi, Marlene Bonmann, et al.

Samu-Ville Pälli, Aleksi Tamminen, Paavo Hiltunen, Sazan Rexhepi, Marlene Bonmann, Tomas Bryllert, Duncan A. Robertson, Juha Ala-Laurinaho, Jan Stake, Zachary Taylor, "Imaging experiments with a 340-GHz FMCW radar and frequency-diverse holograms," Proc. SPIE 12535, Radar Sensor Technology XXVII, 125350M (14 June 2023); doi: 10.1117/12.2663757

SPIE.

Event: SPIE Defense + Commercial Sensing, 2023, Orlando, Florida, United States

Downloaded From: https://www.spiedigitallibrary.org/conference-proceedings-of-spie on 25 Sep 2023 Terms of Use: https://www.spiedigitallibrary.org/terms-of-use

Imaging experiments with a 340-GHz FMCW radar and frequency-diverse holograms

Samu-Ville Pälli[a], Aleksi Tamminen[a], Paavo Hiltunen[a], Sazan Rexhepi[a], Marlene Bonmann[b], Tomas Bryllert[b], Duncan A. Robertson[c], Juha Ala-Laurinaho[a], Jan Stake[b], and Zachary Taylor[a]

[a]Department of Electronics and Nanoengineering, MilliLab, Aalto University, Maarintie 8, 02150 Espoo, Finland
[b]Terahertz and Millimetre Wave Laboratory, Department of Microtechnology and Nanoscience, Chalmers University of Technology, SE-412 96 Gothenburg, Sweden
[c]School of Physics and Astronomy, University of St Andrews, St Andrews, Fife KY16 9SS, UK

ABSTRACT

We present recent developments of a standoff imaging system based on a frequency-diverse phase hologram and deep neural networks. The single-pixel imaging system operates in a monostatic configuration consisting of a 340-GHz FMCW radar and a frequency-diverse phase hologram to interrogate the radar down range direction with spatially varying, frequency-dependent field patterns. The measured back-reflected signal contains spatial reflectivity information from the target, and the fast chirp rate of the radar enables real-time imaging performance. Together with simultaneously acquired visible-light images, a deep neural network integrated into the submillimeter-wave data readout electronics can map the received signal onto a 2D image without mechanical or active electrical beam scanning. In experiments, we have collected submillimeter-wave and visible-light data of a moving target in the region of interest with a 60-Hz frame rate. The results suggest that the system can image the moving target with a resolution comparable to the theoretical diffraction limit. The minimal hardware complexity and good imaging performance of the demonstrated computational submillimeter-wave imaging system support its potential as a cost-effective and easily deployable solution for various imaging applications.

Keywords: Hologram, imaging, FMCW radar, neural network, submillimeter-wave

1. INTRODUCTION

High-resolution images and the ability to penetrate through optically opaque materials highlight the potential of submillimeter waves in a wide range of imaging applications. Many of the imaging scenarios in fields such as medical imaging or security screening often involve moving targets, necessitating high frame rates to capture the target. Conventionally, high frame rates in submillimeter-wave imaging systems require fast beamsteering methods to capture the information from the region of interest (RoI). These methods include mechanical beamsteering [1], where the object plane focal point is scanned over the RoI with rapidly actuated mirrors, and electrical beamsteering [2], applying an array of amplitude or phase shifting elements to manipulate the radiation pattern. Both methods suffer from large footprints and complexity. The number of transceivers in the array also multiplies the cost, especially with submillimeter-wave technology, while mechanical parts require constant maintenance.

Computational imaging methods have demonstrated potential at millimeter- and submillimeter-waves to overcome these drawbacks by simplifying the imaging architecture at the expense of added complexity in signal processing and image reconstruction [3]. Frequency-diverse imaging is a computational imaging technique utilizing antennas or apertures engineered to create complex, spatially varying beam patterns as the frequency is swept over a wide operating bandwidth. As these spatially varying beam patterns interrogate the RoI, the reflectivity information from the target is encoded to the back-reflected signal. Using different image reconstruction techniques, the reflectivity distribution of the RoI can be restored from the complex, wide-band submillimeter-wave signal. This allows imaging frame rates that are not dependent on scanning the beam over the RoI but depend only on the sweep time and computing power at the system back end.

Radar Sensor Technology XXVII, edited by Abigail S. Hedden, Gregory J. Mazzaro, Ann Marie Raynal, Proc. of SPIE Vol. 12535, 125350M · © 2023 SPIE
0277-786X · doi: 10.1117/12.2663757

Downloaded From: https://www.spiedigitallibrary.org/conference-proceedings-of-spie on 25 Sep 2023
Terms of Use: https://www.spiedigitallibrary.org/terms-of-use

Furthermore, frequency-diverse apertures enable imaging using only one transceiver, often referred to as a single-pixel camera [4], further reducing hardware costs. Frequency-diverse apertures have been demonstrated at microwaves, millimeter- and submillimeter-waves using cavity resonators, and passive or active metamaterials [5,6,7]. These methods rely on accurate knowledge of the propagation path to approximate the solution of the image reconstruction inverse problem. Complex aperture designs can create many uncorrelated measurement modes, leading to high-quality images even with smaller bandwidths [8]. Earlier, we have demonstrated the frequency-diverse holograms in localization tasks using a terahertz time-domain spectrometer (THz-TDS) operating at 0.1-2.0 THz and in imaging of moving targets using a vector network analyzer (VNA) at 220-330 GHz [9,10,11].

In this work, we present the recent development and experimental results of a submillimeter-wave standoff imaging system based on frequency-diverse holograms and a 340-GHz frequency-modulated, continuous wave (FMCW) radar. The imaging system uses a single transceiver and a frequency-diverse hologram to illuminate the RoI without mechanical or electrical beamsteering. The back-reflected signal from a moving target is fed into a deep neural network, which is able to reconstruct the image of the target in real time.

2. IMAGING SYSTEM

The imaging system is based on frequency-diverse illumination of the region of interest using a dispersive, transmission-type phase hologram. The hologram is designed to disperse the incident field to the RoI with a strong spatial variation over the 325-355 GHz operating bandwidth. Each frequency point of the back-reflected signal contains a reflectivity distribution of the RoI weighted with the spatial field distribution. Using a fast-chirping FMCW radar, the system is able to interrogate the region of interest over a wide bandwidth in real-time. Combined with the distance information inherent to the FMCW operation, the received complex signal contains enough information from the RoI to enable image reconstruction using neural networks. A visible light camera (Basler acA2440-20gc) is integrated into the radar system to provide ground truth images of the target for the neural network training. The small form factor of the transceiver, quasioptics, and radar electronics make the system portable and easily deployable for various applications. Figure 1 shows the complete imaging system.

Figure 1. The overview of the imaging system. The FMCW radar, hologram, and visible light camera are mounted on a tripod for portability and alignment. The dimensions of the white radar casing are 28 x 33 x 45 cm. The table on the right holds the radar power supply unit and the system PC.

Downloaded From: https://www.spiedigitallibrary.org/conference-proceedings-of-spie on 25 Sep 2023
Terms of Use: https://www.spiedigitallibrary.org/terms-of-use

2.1 Frequency-diverse hologram

The quasirandom surface relief of the hologram is designed to create frequency-diverse radiation patterns over a 0.5 × 0.5 m^2 region of interest at a 1-meter distance following the design process described in [12]. The surface relief is CNC-milled onto a 25-mm thick, 152.4 mm in diameter disc of Rexolite 1422, low-loss cross-linked polystyrene with a relative permittivity of ε_r = 2.52 - j0.0005. [13]. The surface relief consists of seven distinct height levels with a step height of 3.8 mm, corresponding to an electrical path length difference of 6.5 to 7.1 wavelengths at 325 – 355 GHz. To maximize the spatial diversity while minimizing the power loss outside the region of interest, the hologram surface relief is optimized using a spatial filtering technique [14], and the field from the transceiver horn antenna is collimated with a Rexolite hyperbolic lens.

2.2 FMCW radar

To reach the imaging frequencies of 325-355 GHz, the radar uses up-converted and frequency-multiplied chirps generated by direct digital synthesis (DDS) evaluation board (Analog Devices AD9914) clocked at 3.5 GHz using a stable local oscillator. The DDS outputs a 0.9 – 1.4 GHz linear chirp with a 25 µs chirp time. This signal is first mixed to the lower sideband against a 6.5 GHz stable local oscillator. The resulting 5.1 – 5.6 GHz chirp is filtered, amplified, and doubled to 10.2 – 11.2 GHz with a frequency doubler. This X-band signal is further amplified and fed to the transceiver module. The transceiver module consists of a x8 MMIC and two x2 Schottky diode multipliers totaling x32 multiplication of the chirp, resulting in up to approximately 30 GHz bandwidth with 340 GHz center frequency. The transceiver module was initially developed for the CONSORTIS imaging radar [15] by Wasa Millimeter Wave AB and is described in detail in [16]. The final doubling stage of the module acts simultaneously as a sub-harmonic mixer on receive, mixing the received signal with the transmitted signal directly down to the baseband frequency range of around 5-30 MHz. The transceiver module is coupled to a custom smooth-walled spline profile horn antenna, illuminating the hyperbolic lens and the hologram. Figure 2 illustrates the radar electronics in detail.

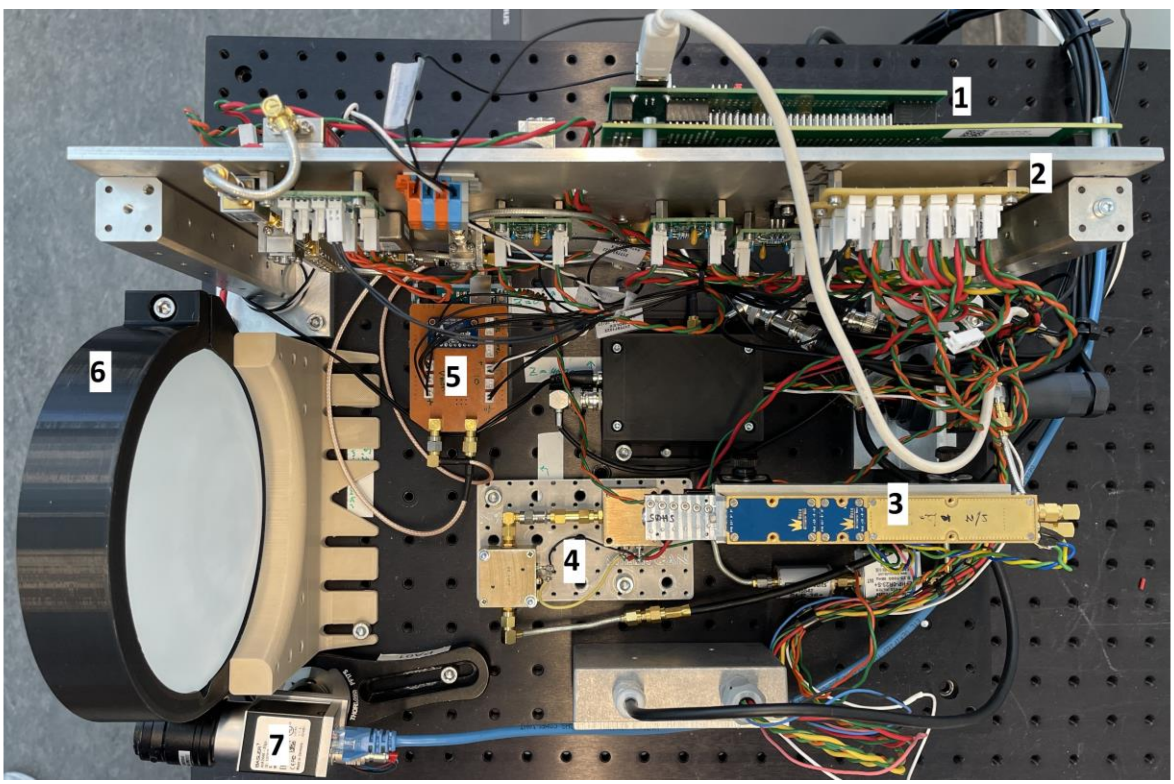

Figure 2. The radar electronics in detail. (1) DDS evaluation board for chirp generation. (2) Aluminum support plate housing the RF and power electronics for up-converting, filtering, and amplifying the chirp. (3) The 340-GHz transceiver module. (4) RF electronics for the received signal. (5) Arduino microcontroller providing the synchronization for the chirp generator, visible light camera, and ADC. (6) Rexolite hyperbolic lens and the hologram. (7) Visible light camera.

Downloaded From: https://www.spiedigitallibrary.org/conference-proceedings-of-spie on 25 Sep 2023
Terms of Use: https://www.spiedigitallibrary.org/terms-of-use

2.3 Signal processing

The filtered and amplified baseband signal from the transceiver module is digitized using one channel of an analog-to-digital converter (ADC) PCIe card (AlazarTech ATS9146) connected to the system PC (Intel I7-11700F, Nvidia RTX 3070, 16 GB RAM). The system PC runs the radar software, data acquisition, signal processing, and the neural network. The ADC has two channels with a sampling rate of 125 megasamples per second with 14-bit resolution. An external trigger signal is generated using an Arduino microcontroller to synchronize the radar chirp, visible light camera shutter, and the ADC data acquisition. The digitized signal and the corresponding visible camera images are streamed to the system PC memory. As the real-valued signal is read from memory, a Hilbert transformation is applied to the signal to get the IQ-formatted complex-valued data. Finally, the IQ components of the signal are min-max normalized for the neural network input.

At this stage, the signal can be fed into a trained neural network for image reconstruction or used to train the neural network on the fly. When training the neural network on the fly, the system takes in chunks of 110 signal and visible camera image pairs (100 for training, 10 for validation) to continuously train the neural network for image reconstruction, while displaying one predicted image along with the network parameters every two seconds for the user to monitor the convergence of the training. If the signal is fed into a pre-trained neural network, the system is able to output the predicted image approximately every 16 milliseconds, resulting in a 60-Hz frame rate.

2.4 Neural network

The neural network used in image reconstruction is discussed in detail in [10]. The filtered, transformed, and normalized signal was mapped into an image through a deconvolutional neural network. The input data is reshaped into 2×2 layers consisting of 1000 channels in total. The 2×2 layer is sequentially deconvoluted (transpose convolutional layer) with a kernel size of 3×3 and stride of 2 in both dimensions. The output of each deconvolutional layer is padded with "same". This process doubles the layer size in both dimensions on each deconvolution at the same time as the number of channels is gradually reduced. After six deconvolutional layers, the layer size is 64×64, and one channel, which is the predicted image. The activation functions in each deconvolutional layer are rectified linear units (ReLU) except for the sigmoid function at the output. The visible-light camera images are down-sampled to 64×64 pixels and blurred to correspond to the diffraction-limited spot size of about 10 mm. The loss function is the categorical cross-entropy. The hyper-parameters of the neural network are the learning rate of 0.001 and $p = 50\%$ in the dropout layer at the beginning of the neural network. The neural network was trained with the Keras machine-learning API running in real-time and accumulating the data continuously.

3. IMAGING EXPERIMENT AND RESULTS

3.1 Imaging setup

The imaging setup in the experiment consists of the presented imaging system and an aluminum optical chopper blade as a target in the RoI. The rotating chopper blade is mounted on another tripod at a 1-meter distance from the imaging system. A 20-cm tall Styrofoam block elevates the chopper and its mount to reduce unwanted reflections from the tripod legs. The background wall is covered with radar-absorbing material to minimize multiple reflections. Figure 3 illustrates the imaging setup. Using the chopper blade controller, the blade is set to rotate at a speed of two complete rotations per second. The imaging system is pointed towards the chopper blade using the visible camera feed from the radar system software.

3.2 Training data

The imaging system is used to interrogate the chopper blade with the FMCW radar for approximately 10 minutes while the neural network is trained on the fly, resulting in roughly 36 000 received signals and corresponding visible light images. The signal received by the radar is IQ-formatted using the Hilbert transform, normalized to [-1, 1] interval, and used as an input to the neural network. The labels for the neural network are the visible light images converted to black-and-white, downscaled to 64 x 64 pixels, and blurred using a 5 x 5-pixel Gaussian filter. The filtering is used to downscale the visible camera detail sharpness to levels comparable to the diffraction-limited resolution at 325-355 GHz. Examples of the neural network input data and labels are shown in Figure 4 (a and c).

Downloaded From: https://www.spiedigitallibrary.org/conference-proceedings-of-spie on 25 Sep 2023
Terms of Use: https://www.spiedigitallibrary.org/terms-of-use

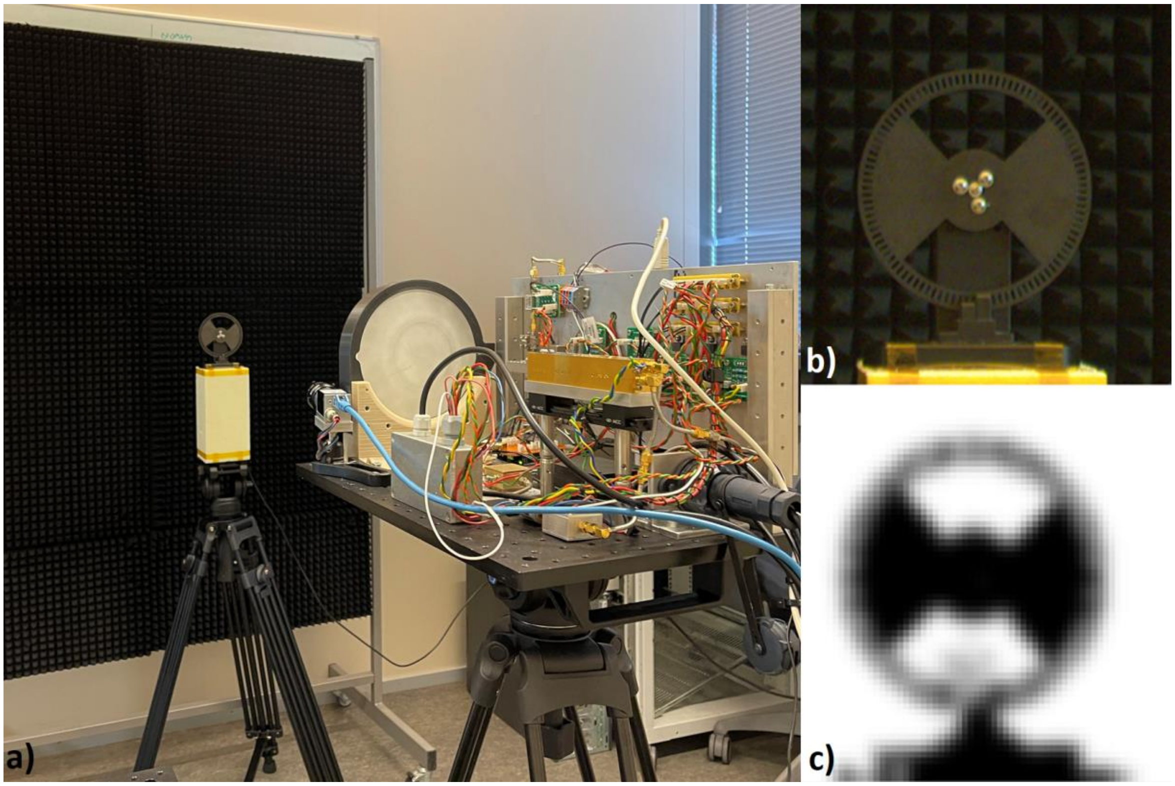

Figure 3. a) The overview of the imaging setup. b) Visible light camera image of the chopper blade target. c) Gaussian blurred 64 x 64-pixel black-and-white image used as ground truth for the neural network.

3.3 Imaging results

After the ten-minute training phase, the neural network is left to run and constantly predict the chopper blade position, while the blade is still rotating at the speed of two rotations per second. The system is capable of updating the predicted image with a 60-Hz frame rate. Figure 4 shows two examples of predicted images (b and e) along with the corresponding signals (a and d) and ground truth images (c and f). Comparing the predictions and ground truth images, it is evident that the neural network can predict the blade orientation from the received radar signal. The blur around the blade edges indicates some uncertainty in the prediction but also suggests that the neural network is not overfitted, i.e., has not memorized every possible blade orientation.

Looking at the IQ representations in Figure 4 a) and d) (top), the difference in the signal between different blade orientations is not visible to the eye. Still, the results suggest that the neural network is able to separate the relevant information from the signal. The differences are more discernible in the frequency-domain a) and d) (bottom). The region of interest at a one-meter distance corresponds to approximately 11 MHz frequency in the received baseband signal. Moreover, the complex hologram surface relief seems to spread the chirp in time, as there are apparent differences in the frequency-domain signal over a range of 11 to 14 MHz between the two blade orientations. This is a promising result concerning future imaging experiments with different targets, indicating that the hologram can create a different spectral fingerprint at the baseband frequencies based on the spatial features of the target.

Downloaded From: https://www.spiedigitallibrary.org/conference-proceedings-of-spie on 25 Sep 2023
Terms of Use: https://www.spiedigitallibrary.org/terms-of-use

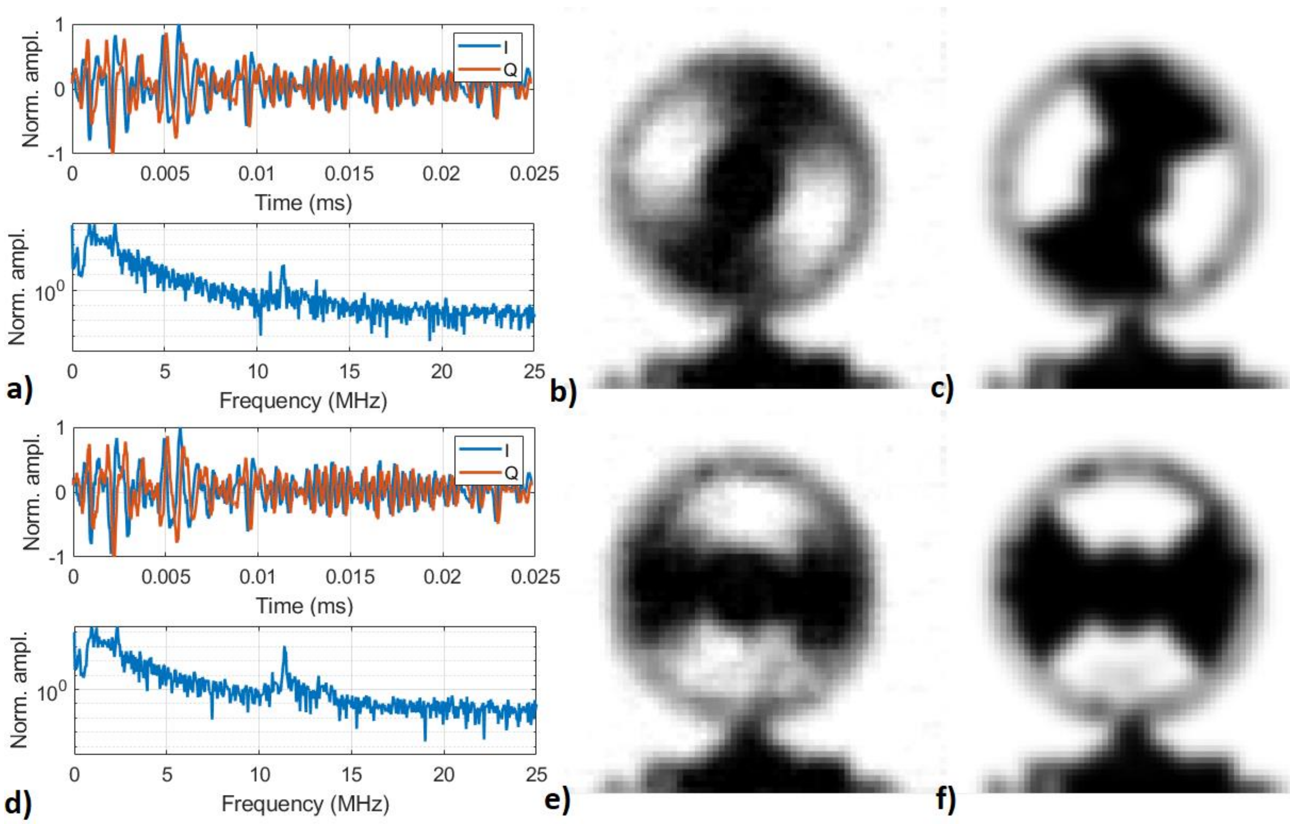

Figure 4. a) Received IQ-formatted time-domain signal from the target (up). This signal is used as an input to the neural network. Corresponding frequency-domain representation of the signal (bottom). b) Predicted image of the target generated by the neural network. c) Gaussian-filtered visible light black-and-white image of the target. d-f) Corresponding result for a different chopper blade orientation.

4. CONCLUSIONS

We have presented experimental results of a submillimeter-wave imaging system based on frequency-diverse phase holograms and image reconstruction using neural networks. The imaging system uses an FMCW radar illuminating the hologram to interrogate the region of interest with spatially varying beam patterns at 325-355 GHz. The received signal contains information on the spatial reflectivity distribution of the RoI weighted by the different field patterns at each frequency. The imaging system has an integrated visible light camera to capture the ground truth image of the target. We have trained a neural network for image reconstruction by interrogating a rotating optical chopper blade with submillimeter waves while simultaneously acquiring visible light images of the target. After a short training period, the neural network can reconstruct the image with reasonable accuracy by predicting the orientation of the chopper blade from the received radar signal. The results suggest that the imaging system can extract spatial features from the region of interest based on the spectral fingerprint in the received signal. The research continues towards training different targets with various shapes for the neural network and their detection when concealed. We believe the presented imaging system enables an efficient and easily deployable imaging solution for various imaging applications.

ACKNOWLEDGMENTS

This work is supported by the Business Finland research to business project R2B-MilliScan. Aalto Design Factory is thanked for the manufacturing of the quasioptics. Mr. Markus Grönholm from Alshain Oy is thanked for manufacturing the hologram and radar software development.

Downloaded From: https://www.spiedigitallibrary.org/conference-proceedings-of-spie on 25 Sep 2023
Terms of Use: https://www.spiedigitallibrary.org/terms-of-use

REFERENCES

[1] K. B. Cooper, R. J. Dengler, N. Llombart, B. Thomas, G. Chattopadhyay, and P. H. Siegel, "THz Imaging Radar for Standoff Personnel Screening," *IEEE Trans. THz. Sci. Technol.,* vol. 1, no. 1, pp. 169-182, 2011.

[2] S. S. Ahmed, A. Schiessl, and L.-P. Schmidt, "A Novel Fully Electronic Active Real-Time Imager Based on a Planar Multistatic Sparse Array," *IEEE Trans. Microw. Theory Techn.,* vol. 59, no. 12, pp. 3567-3576, 2011.

[3] O. Yurduseven, T. Fromenteze, K. Cooper, G. Chattopadhyay, and D. Smith, "From microwaves to submillimeter waves: modern advances in computational imaging, radar, and future trends," *Proc. SPIE 10917, Terahertz, RF, Millimeter, and Submillimeter-Wave Technology and Applications XII,* Mar. 2019, Art. no. 1091710.

[4] R. I. Stantchev, X. Yu, T. Blu, and E. Pickwell-MacPherson, "Real-time terahertz imaging with a single-pixel detector," *Nat. Commun.,* vol. 11, pp. 1-8, 2020.

[5] T. Fromenteze, O. Yurduseven, M. F. Imani, J. Gollub, C. Decroze, D. Carsenat, and D. R. Smith, "Computational imaging using a mode-mixing cavity at microwave frequencies," *Appl. Phys. Lett.* vol. 106, no. 19, 2015.

[6] T. Zvolensky, V. R. Gowda, J. Gollub, D. L. Marks, and D. R. Smith, "W-Band Sparse Imaging System Using Frequency Diverse Cavity-Fed Metasurface Antennas," *IEEE Access,* vol. 6, pp. 73659-73668, 2018.

[7] S. Venkatesh, X. Lu, H. Saeidi, and K. Sengupta, "A high-speed programmable and scalable terahertz holographic metasurface based on tiled CMOS chips," *Nat. Electron.* vol. 3, pp. 785-793, 2020.

[8] O. Yurduseven, J. Gollub, D. L. Marks, and D. R. Smith, "Frequency-diverse microwave imaging using planar Mills-Cross cavity apertures," *Opt. Express,* vol. 24, no. 8, pp. 8907-8925, 2016.

[9] A. Tamminen, S.-V. Pälli, J. Ala-Laurinaho, A. Aspelin, A. Oinaanoja, and Z. Taylor, "Holograms with neural-network backend for submillimeter-wave beamforming applications," *Proc. SPIE 11411, Passive and Active Millimeter-Wave Imaging XXIII,* Apr. 2020, Art. no. 114110C.

[10] A. Tamminen, S.-V. Pälli, J. Ala-Laurinaho, and Z. D. Taylor, "Millimeter- and Submillimeter-Wave Imaging Through Dispersive Hologram and Deep Neural Networks," *IEEE Trans. Microw. Theory Techn.,* vol. 70, no. 6, pp. 3281-3290, 2022.

[11] S.-V. Pälli, P. Hiltunen, M. Kosonen, A. Tamminen, J. Ala-Laurinaho, and Z. Taylor, "Submillimeter-wave holograms and imaging neural network: experiments at 220-330 GHz," *Proc. SPIE 12111, Passive and Active Millimeter-Wave Imaging XXV,* Jun. 2022, Art. no. 1211109.

[12] S.-V. Pälli, A. Tamminen, J. Ala-Laurinaho, and Z. D. Taylor, "Design and Characterization of Phase Holograms for Standoff Localization at Millimeter and Submillimeter Waves," *IEEE Trans. Microw. Theory Techn.,* vol. 70, no. 1, pp. 907-918, 2022.

[13] J. W. Lamb, "Miscellaneous data on materials for millimetre and submillimetre optics," *J. Infrared Millim. Waves,* vol. 17, no. 12. pp. 1997-2034, 1996.

[14] S.-V. Pälli, A. Tamminen, J. Ala-Laurinaho, S. Rexhepi, and Z. Taylor, "Frequency-diverse phase holograms with spatial filtering for submillimeter-wave imaging," *2023 47th International Conference on Infrared, Millimeter and Terahertz Waves (IRMMW-THz), Montreal, Canada,* 2023. [Submitted]

[15] D. A. Robertson *et al.,* "A high frame rate, 340 GHz 3D imaging radar for security," *2018 IEEE Radar Conference (RadarConf18),* Apr. 2018, pp. 0055-0060.

[16] R. Dahlbäck, T. Bryllert, G. Granström, M. Ferndahl, V. Drakinskiy, and J. Stake, "Compact 340 GHz homodyne transceiver modules for FMWC imaging radar array," *2016 IEEE MTT-S International Microwave Symposium (IMS),* 2016, pp. 1-4.

Downloaded From: https://www.spiedigitallibrary.org/conference-proceedings-of-spie on 25 Sep 2023
Terms of Use: https://www.spiedigitallibrary.org/terms-of-use